ION SIMULATIONS, RECENT UPGRADES AND TESTS WITH TITAN'S COOLER PENNING TRAP

R. Silwal[1,*], S. F. Paul[1,2], B. K. Kootte[1,3], T. Joseph[1,4], R. Simpson[1,5],
A. A. Kwiatkowski[1,6], G. Gwinner[3], J. Dilling[1,4], and the TITAN collaboration

[1] TRIUMF, Vancouver, BC Canada
[2] Ruprecht-Karls-Universität, Heidelberg, Germany
[3] University of Manitoba, Winnipeg, MB Canada
[4] University of British Columbia, Vancouver, BC Canada
[5] University of Waterloo, Waterloo, ON Canada
[6] University of Victoria, Victoria, BC Canada

Abstract

TRIUMF's Ion Trap for Atomic and Nuclear science (TITAN) facility has the only on-line mass measurement Penning trap (MPET) at a radioactive beam facility that uses an electron beam ion trap (EBIT) to enhance mass precision and resolution. EBITs can charge breed exotic isotopes, making them highly charged, thereby improving the precision of atomic mass measurement as the precision scales linearly with the charge state. However, ion bunches charge bred in the EBIT can have larger energy spread, which poses challenges for mass measurements. A cooler Penning trap (CPET) is currently being developed off-line at TITAN to sympathetically cool the highly charged ions (HCI) with a co-trapped electron plasma, prior to their transport to the MPET. To evaluate the integration of the CPET into the TITAN beamline and to optimize the beam transport, ion trajectory simulations were performed. Hardware upgrades motivated by these simulations and previous test measurements were applied to the off-line CPET setup. Ions and electrons were co-trapped for the first time with the CPET. Progress and challenges on the path towards HCI cooling and integration with the on-line beam facility are presented.

INTRODUCTION

Atomic mass measurements of short-lived radioactive isotopes are useful to study nuclear structure, test existing nuclear models, explore the nuclear astrophysics reaction paths, and test predictions of fundamental physics beyond the Standard model [1–4]. TRIUMF's Ion Trap for Atomic and Nuclear Science (TITAN) facility [5], is dedicated to high precision mass measurements as well as in-trap decay spectroscopy of radioactive ion beams (RIB). The TITAN system (see Fig. 1) is comprised of the following ion traps:

- A radio-frequency quadrupole (RFQ) cooler and buncher,
- A measurement Penning trap (MPET),
- An electron beam ion trap (EBIT),
- A cooler Penning trap (CPET), and
- A multiple-reflection time-of-flight mass spectrometer (MR-TOF MS)

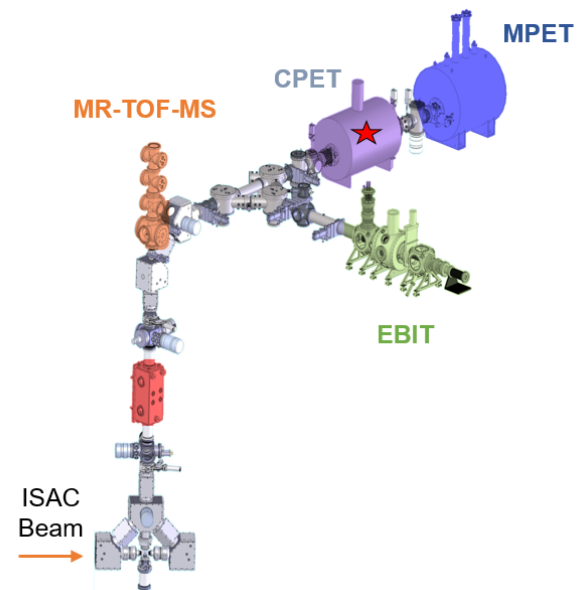
* roshanisilwal@gmail.com

Figure 1: The TITAN beamline shown with different traps color-coded (the star indicates that the trap is not currently coupled to the radioactive beamline).

The RFQ cooler and buncher [6] receives the radioactive beam from the isotope separator and accelerator (ISAC) facility [7] at TRIUMF at a beam energy of 20 keV. It then cools the ions via collisions with He buffer gas, and bunches the beam. Downstream of the RFQ, a pulsed drift tube reduces the energy of the ion bunches to roughly 2 keV to match the acceptance of the other ion traps. The MR-TOF MS [8,9] is used to either clean isobaric contaminants from the radioactive beam or for highly sensitive mass measurements and is advantageous for low-intensity or highly contaminated RIB species. TITAN-MPET [10] can perform extremely precise mass measurements using a time-of-flight ion-cyclotron-resonance (ToF-ICR) method [11,12] by measuring the cyclotron frequency (ν_c) of the ion. Since $\nu_c = qB/2\pi m$, the mass values can be extracted from ν_c. For singly charged ions, the MPET has achieved ppb precision [10], which is sufficient for nuclear structure and astrophysics studies. However, in order to test fundamental symmetries, an even high precision can be required [13].

The mass measurement precision in the MPET is limited by the charge state of the species (q), the number of ions observed during the measurement (N_{ions}), the RF excitation time (T_{rf}), and the magnetic field (B) as shown in Eq. (1).

$$\frac{\delta m}{m} = \frac{m}{qBT_{rf}\sqrt{N_{ions}}}. \qquad (1)$$

Of these parameters, the superconducting magnet of 3.7 T is fixed, N_{ions} depends on the measurement cycle time, the RIB production rate and the contaminants, and (T_{rf}) is limited by the half-life of the exotic ions. The charge state of the species can be increased to enhance the mass precision and resolving power [14–17]. TITAN has the only on-line Penning trap at a RIB facility, coupled to the EBIT to charge breed ions in order to increase the charge state [4, 18–22]. The highly charged ions (HCI) can charge-exchange with neutral atoms in the MPET, damping and/or shifting the ToF-ICR resonances [23], hence deteriorating mass precision and resolving power. To reduce the probability of charge-exchange, TITAN-MPET is currently being upgraded to a cryogenic trap which will significantly reduce the residual gas level.

Currently, TITAN-EBIT [24, 25] can operate at 65 keV beam energy, 500 mA electron beam current, and 6 T magnetic field. The existing electron gun will be upgraded to a newly designed system that can provide up to 6 A beam current. Singly charged ions transported to the EBIT are ionized to high charge states by electron impact ionization. The electron beam is compressed to roughly 100 µm radius by the 6 T field as it passes through the trapping region that consists of several drift tubes. These HCI are axially trapped by an electric field applied across the drift tube electrodes and radially confined by the combined effects of the magnetic field and the space-charge of the electron beam. These charge-bred ions are then extracted by an extractor electrode at the collector region and transported to the MPET for mass measurements.

The transversal and longitudinal emittance of ion bunches extracted from the EBIT can exceed the acceptance of the MPET. The ~20 eV/q energy spread of the highly charged ion beam [26] extracted from the EBIT can lead to reduced injection efficiency and smeared TOF resonances. The mass precision is reduced as the ions probe a larger volume in the trap and therefore more magnetic field inhomogeneities. For maximal mass precision, it is essential to cool the HCI bunch before extraction in order to reduce its energy spread. Most of the available cooling techniques such as buffer cooling [27] and optical cooling [28] do not apply to HCIs due to the large charge exchange cross-sections and limited availability of appropriate atomic transitions for laser cooling. In an effort to cool HCIs, a practical solution based on electron cooling [29,30] is being pursued at TITAN. HCIs are cooled by Coulomb collisions between ions and electrons that self cool in the 7 T magnetic field through emitting cyclotron radiation [31, 32].

The CPET [33] consists of 29 cylindrical trap electrodes where both ions and electrons are trapped simultaneously in nested potential wells. A schematic of the CPET is shown in Fig. 2. The gate electrodes (G1, G2) confine injected electrons which then cool into the nested positive potential well. The pulsed drift tube (DT1) is used to reduce the energy of incoming ion bunches from ~ 2 keV to a few 10 eV thus making them trappable within the CPET. After the cooling process, the energy of extracted ion bunches is elevated with another pulsed drift tube (DT2) for transport to the MPET. The off-line setup comprises an ion source to inject stable singly charged ions into the trap which will be replaced by the EBIT in the on-line system. Several efforts were made in optimizing the trap, characterizing the electron plasma, enhancing electron injection, and improving the beam diagnostics. The most important developments include the design of an off-axis electron gun for electron injection that provides an unobstructed extraction of cooled ions towards the MPET [34], and a harp detector [35] built to diagnose the electron plasma without obstructing the transport of the ions into the trap.

Previous studies with the CPET have provided insight into plasma instabilities and oscillation modes that may be enhanced by asymmetries in the system [31]. This study revealed ~minute trapping times and suggested that even longer trapping times without losing the plasma can be achieved by applying a counteracting rotating wall drive [36]. Successful electron plasma creation was demonstrated using an on-axis [34] and off-axis [37] electron gun with the first signs of self-cooling in electrons. Characterizing the ion trapping, however, posed a challenge due to high voltage sparks/discharges in the system. With many electrodes, a compact vacuum feed-through wiring section, and high voltage switching among multiple electrodes, the system is fairly complex. Motivated by a need to simplify the setup and to optimize the ion-electron dynamics, we performed ion trajectory simulations followed by a few hardware changes in the system. Here, we present the current status, recent results, and upgrades of the off-line CPET setup. We also discuss the challenges and upcoming plans for commissioning and online integration into the TITAN beamline.
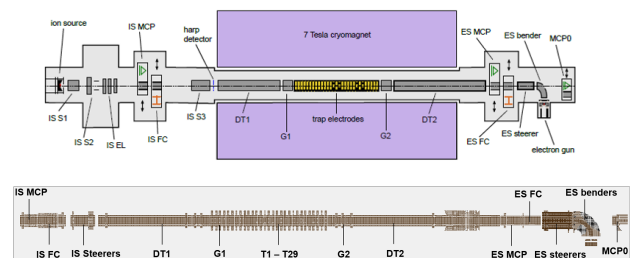

Figure 2: Schematic of the CPET [38] (top) and SIMION geometry shown without the ion source (bottom).

ION TRAJECTORY SIMULATIONS

The ion trajectory simulations were performed using the SIMION package [39], which incorporated both electric and

magnetic fields to understand the beam properties during ion injection and extraction. Previously, the 29 trap electrodes were floated to 1 kV or higher during normal operation, potentially leading to HV discharges. To avoid this, we developed a new scheme with the trap near ground potential. This scheme adds a complication of having to pulse the drift tube (DT1) to inject the ions. The first goal of the simulations was to find suitable settings for ion injection with the new scheme. To do so, a simulated 2 keV ion beam, with ~20 eV energy spread was injected into the trap using the SIMION geometry. DT1 was pulsed from +1 kV to −1 kV during injection to reduce the beam energy. Strong accelerating negative voltage was required to avoid magnetic field reflection when the ion beam enters the high B regime and to maximize the beam transmission.

Upon interaction with the self-cooled electrons, the ions would cool in the 2 ion wells next to the end caps as seen in Fig. 3. The cooled ions will be extracted from one of the wells by lowering the end cap (E2). Assuming the ion bunches cool to ~ 1 eV, the second goal of the simulations was to obtain an extracted beam with small energy spread and a time focus (i.e. longitudinally compressed bunches) in the MPET (or on the off-line detector). The ions were initialized at the ion well position as a cylindrical beam of a finite length (ranging from 1 to 3 trap electrodes) and a radius of 0.5 mm. Uniform energy spread averaging to ~1 eV/q was used, assuming cold ions, and the extraction of the cooled beam was optimized accordingly. It was found that applying a voltage gradient across a few electrodes is an ideal way of extracting the ion bunch without adding additional energy spread. Extracted ion bunches were brought to a suitable transport energy of 2 keV by pulsing drift tube DT2 from −1 kV to +1 kV. The simulations showed that pulsing the DT2 bias with appropriate timing did not affect the beam energy spread.

Figure 3 shows the on-axis potential on the trap electrodes optimized for trapping ions. Proper analysis of the applied voltages was required since the trap electrodes were affected by the field penetration of the nearby gate electrodes. In order to account for this field penetration, three trap electrodes on either end of the gate electrodes were set to the same potential and used as end cap electrodes to trap the ions. Two modes of extraction, shown in Fig. 3 (bottom), produced good beam properties. The optimum condition was obtained when a linear voltage gradient along four trap electrodes was created (red). Pulsing a few electrodes to a constant negative potential (blue) also resulted in ~2 eV energy spread of the extracted ion bunch.

The third goal of the simulations was to check if the TOF signal on the off-line detector on the electron side (ES MCP0) could be used to probe changes in beam energy of cooled (1 eV/q) bunches versus uncooled (20 eV/q) bunches. An energy spread of ~1 eV and a time focus of 200 ns were achieved for the cold beam. Figure 4 shows a Gaussian fit for the energy spread of the extracted beam with and without cooling.
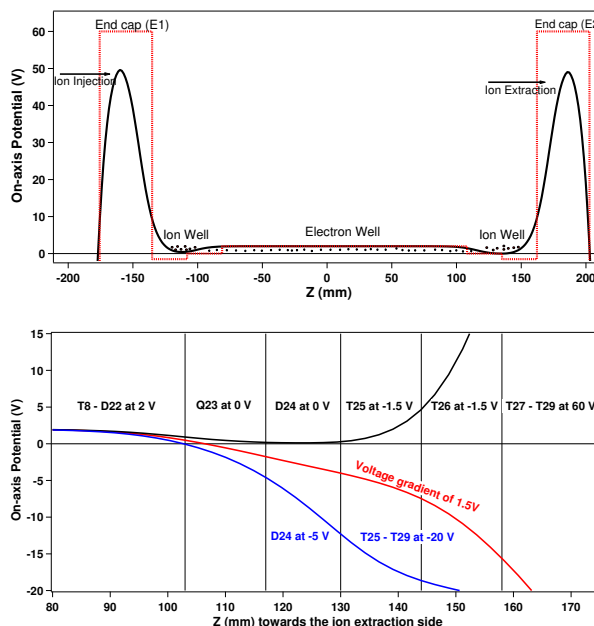

Figure 3: On-axis potential during ion trapping in black and the applied voltages in red (top) and extraction with a linear voltage gradient in red and fixed potential in blue (bottom). Note the trap center is located at z = xy; labels T, D and Q refer to the type of the trap electrode (unsegmented ring electrode, two-fold segmented dipole electrode and 4-fold segmented quadrupole electrode).
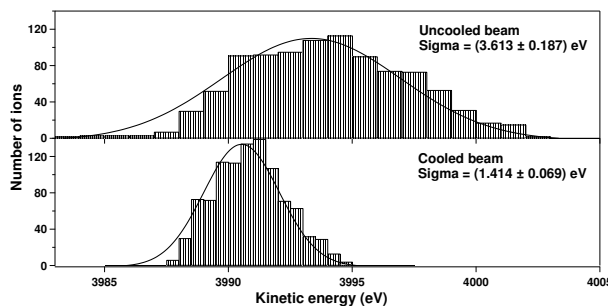

Figure 4: Energy spread of the extracted ions (here the MCP biased at −2 kV to image the beam) for cooled vs uncooled ions (from simulations). The uncooled beam has larger energy spread as expected.

The positive simulation results motivated the realization of the above operation scheme for the CPET. To this end with the goal of increased robustness against HV discharges in mind and to accommodate the simulation results, the following hardware changes were applied to the system. The three trap electrodes on either end of the gate electrodes were biased with the same voltage. The respective segments of several azimuthally split electrodes were shorted within the vacuum chamber, hence reducing the number of HV carrying cables within the magnet bore. Among them were a pair of dipoles forming a regular trap electrode and the adjacent electrodes in the two octupoles to form quadrupoles. The first quadrupole was kept at the trap center to apply the

rotating wall drive to the electrons. The second quadrupole was moved to the ion extraction end, where the potential minimum of the trap occurs, with a set of dipole electrodes on either side to allow for mass selective dipole cleaning [31]. The careful arrangement of electrode wires allowed maximum spacing between HV-carrying wires. The ones requiring high voltage switching were placed closer to the outer chamber to avoid possible sparking. The ceramic tubes surrounding the copper wires and the wire lengths were changed according to the new trap configuration to avoid open wire ends. As motivated by the simulation results, a resistor chain for the creation of linear voltage gradients was built.

CHARACTERIZING THE ELECTRON AND ION TRAPPING

Electron Plasma Studies

First tests of trapping and detection of over 10^8 electrons were reported in [40], using an on-axis electron gun. Further tests with an upgraded off-axis electron gun [34] were performed to quantify electron loading and trapping. Recent tests were conducted with a typical emission current of 70 µA that resulted in a DC current of ~1 µA at the harp detector. Loading and trapping were optimized to allow maximum transmission and storage times inside the magnetic field. A scan of the number of trapped electrons at various storage times recorded by the harp detector is shown in Fig. 5, for a 3 s loading time. We achieved a storage time of over 3 minutes, much longer compared to any previous tests. The initial increase in the electron number is due to the damping of an azimuthal asymmetry related m=1 diocotron motion caused by a E × B drift [37, 40]. Early studies by Chowdhury *et al.* [37] showed that the radial displacement of the plasma column recorded on a phosphor screen (inside the magnet bore) decreased on a timescale of 2 s due to this damping. Additionally, the extraction through the diverging magnetic field lines amplifies the initial radial displacement of the plasma and can cause electrons to get lost against the electrode surfaces (of DT1) before reaching the detector.

Longer electron storage times will be necessary when the CPET is coupled with the charge bred HCI and the MPET for mass measurements. Since faster electron cooling requires a large ratio between the number of electrons and ions, and high electron density in the trap [32], the trap was re-loaded to maintain a number of 10^8 trapped electrons or higher with shorter loading times (few hundred ms) for electron related studies. As detailed in [34], we deploy a continuous electron loading mechanism first described by [41]. Electrons were successfully confined in nested potential wells of various shapes formed with the 15 central trap electrodes, thus confirming the self-cooling of electrons in the magnetic field. This was achieved using a floating 16 channel digitally controlled voltage (DAC) supply box developed using a Raspberry Pi controlled Analog Devices evaluation board.

Electron plasma is known to have plasma instabilities triggered by asymmetries in the setup such as misalignments
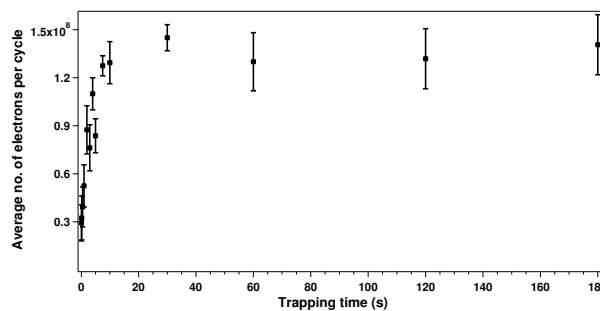
Figure 5: More than 10^8 electrons were trapped for over 3 minutes with an electron loading of 3 s.

in the magnetic and optical axes, off-axis plasma injection, residual gas in the trap, interactions with ions, and application of dipole excitations [42]. Various plasma oscillation modes (radial, azimuthal, and axial) related to the plasma rotations, instabilities, and temperatures exist [43]. The diocotron mode created by the interaction of electrons with their image charge can move the plasma away from the axis leading them to diffuse radially. A counteracting force, created by a rotating-wall drive [36, 42] is needed to ensure a centered plasma with even longer storage times. Another plasma mode in the axial direction, termed the TrivelPiece-Gould mode [43] can be used to diagnose the plasma temperature. Currently, efforts are underway to extract additional information about the electron plasma from the image currents that these plasma oscillations induce on the trap electrodes.

Ion Trapping

A Na surface ion source was used to inject ions into the trap. The ion source emitted a range of ion species that were chopped and steered by a set of electrostatic Lorentz steering elements. Ions of 2 keV energy were reduced to ~100 eV in the drift tube, before sending them to another Lorentz steerer placed inside the magnetic field. These steerers were primarily used to localize the beam in the center of the trap. The three shorted trap electrodes on either end (E1 and E2) were used to trap these ions. By lowering the E2 potential after the desired trapping time, the ions were extracted and recorded by a MCP detector at the end of the beamline. A scan of ion counts for different storage times resulted in a lifetime of nearly 3 s, as shown in Fig. 6. This is the first demonstration of successful ion trapping with the CPET.
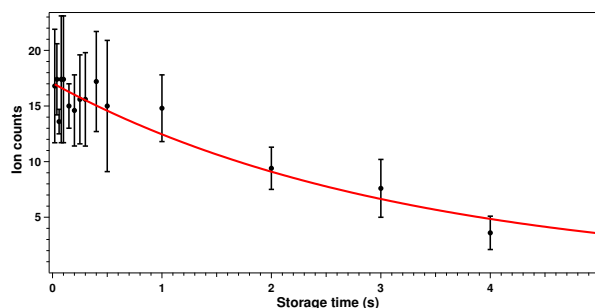

Figure 6: Ions were trapped for several seconds in the trap.

Co-trapping Ions and Electrons

Once the ions and electrons were successfully trapped for reasonably long times, the next steps involved trapping both species simultaneously and evaluating the co-trapping of the two species. The electron/ion loading, trapping, and extraction operation required a robust control to execute these steps. As such, we upgraded the programmable pulse generator software that controls the TTL logic and updated the controls for the power supplies to a Labview interface. It was found that rapid switching of electrode voltages with Behlke HV switches increased the likelihood for HV discharges. Therefore, the rise and fall times of the switches were increased from <50 ns to 300 ns – 1 μs by adding appropriate resistance in series with the HV switches.

Following these improvements to the system, we performed several tests of co-trapping electrons and ions in the CPET. A schematic of the on-potential during the measurements at different CPET electrode positions is shown in Fig. 7. While we successfully detected the presence of both
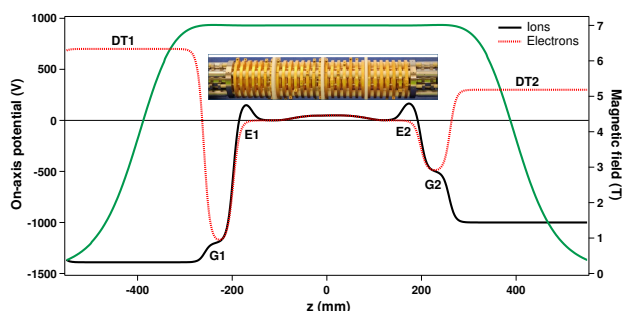

Figure 7: On-axis potentials during the measurements for ions(black solid) and electrodes (red dotted) along with the magnetic field strength (green).

trapped ions and electrons when injected simultaneously, no clear signs of ion cooling have been observed. To observe the signs of cooling, we monitored the TOF signal on the MCP, where the cooled ions are expected to have a longer ToF. We also used the DAC box to bias the trap electrode in the ion extraction end for use as an improvised retarding field analyzer to block ions with lower kinetic energy. A decrease in the energy spread of the extracted ions will provide a clear indication of cooled ions. Challenges faced during these tests include a broad energy profile of the injected ions from an ion source, multiple mass species emitted from the source, and generation of spurious ion signals in the trap when electrons are present. The latter is either caused by electron-impact ionization when electrons collide with the residual gas or is an indication of plasma-induced discharge. Unfortunately, the TOF of the spurious ion counts coincided with the injected ion counts, hence prohibiting a clear indication of cooling. Further studies by adding a Wien filter or a Bradbury-Nielsen gate [44, 45] to the system is needed to identify the masses of the observed signal. Additionally, the resistor chain will be added in the extraction electrodes to improve the beam profile of the extracted ions. A systematic

study of the spatial overlap of the two species will also be conducted as the overlap is needed for maximum cooling power.

CONCLUSION AND OUTLOOK

Ion trajectory simulations and hardware modifications were performed to optimize the beam transmission and minimize high voltage discharge. Electrons and ions were trapped simultaneously with the TITAN-CPET. Systematic studies of charged particle transport and trapping were performed to optimize loading and transmission efficiency. To improve the trapping settings and gain more control when co-trapping both species, and ultimately achieve cooling of ions, several tests are ongoing and planned. These include improving the ion extraction to achieve better time focus, applying the rotating wall drive to store plasma for a longer time and improve plasma compression, diagnosing the source of spurious electron-induced ion signals, and confirming the spatial overlap of the two species. Additionally, an in-situ plasma generation scheme by applying an RF excitation to a CPET electrode is currently being tested.

ACKNOWLEDGEMENTS

REFERENCES

[1] K. Blaum, "High-accuracy mass spectrometry with stored ions", *Phys. Rep.*, vol. 425, no. 1, pp. 1-78, 2006. doi:10.1016/j.physrep.2005.10.011

[2] K. Blaum, J. Dilling, and W. Nörtershäuser, "Precision atomic physics techniques for nuclear physics with radioactive beams", *Phys. Scr.*, vol. 2013, p. 014017, 2013. doi:10.1088/0031-8949/2013/T152/014017

[3] J. Dilling *et al.*, "Mass measurements on highly charged radioactive ions, a new approach to high precision with TITAN", *Int. J. Mass Spectrom.*, vol. 251, pp. 198–203, 2006. doi:10.1016/j.ijms.2006.01.044

[4] A. A. Kwiatkowski *et al.*, "Precision mass measurements at TITAN with radioactive ions", *Nucl. Instrum. Methods Phys. Res., Sect. B*, vol. 317, pp. 517–521, 2013. doi:10.1016/j.ijms.2006.01.044

[5] A. A. Kwiatkowski *et al.*, "TITAN: An ion trap facility for on-line mass measurement experiments", *Hyperfine Interact.*, vol. 225, pp. 143–155, 2014. doi:10.1007/s10751-013-0892-8

[6] T. Brunner *et al.*, "TITAN's digital RFQ ion beam cooler and buncher, operation and performance", *Nucl. Instrum. Methods Phys. Res., Sect. A*, vol. 676, pp. 32–43, 2012. doi:10.1016/j.nima.2012.02.004

[7] M. Dombsky *et al.*, "Commissioning and initial operation of a radioactive beam ion source at ISAC", *Rev. Sci. Instr.*, vol. 71, p. 978, 2000. `doi:10.1063/1.1150364`

[8] C. Jesch *et al.*, "The MR-TOF-MS isobar separator for the TITAN facility at TRIUMF", *Hyperfine Interact.*, vol. 235, pp. 97–106, 2015. `doi:10.1007/s10751-015-1184-2`

[9] E. Leistenschneider *et al.*, "Dawning of the $N = 32$ Shell Closure Seen through Precision Mass Measurements of Neutron-Rich Titanium Isotopes", *Phys. Rev. Lett.*, vol. 120, p. 062503, 2018. `doi:10.1103/PhysRevLett.120.062503`

[10] M. Brodeur *et al.*, "New mass measurement of ^{6}Li and ppb-level systematic studies of the Penning trap mass spectrometer TITAN", *Phys. Rev. C*, vol. 80, p. 044318, 2009. `doi:10.1103/PhysRevC.80.044318`

[11] G. Gräff, H. Kalinowsky, and J. Traut, "A direct determination of the proton electron mass ratio", *Zeitschrift für Physik A: Atoms and Nuclei*, vol. 297, p. 35–39, 1980. `doi:10.1007/BF01414243`

[12] G. Bollen, R. B. Moore, G. Savard, and H. Stolzenberg, "The accuracy of heavy-ion mass measurements using time of flight-ion cyclotron resonance in a Penning trap", *J. Appl. Phys*, vol. 68, p. 4355, 1990. `doi:10.1063/1.346185`

[13] M. P. Reiter *et al.*, "High-precision Q_{EC}-value measurement of the superallowed β^+ emitter ^{22}Mg and an *ab initio* evaluation of the $A = 22$ isobaric triplet", *Phys. Rev. C*, vol. 96, p. 052501(R), 2017. `doi:10.1103/PhysRevC.96.052501`

[14] I. Bergström, "SMILETRAP—A Penning trap facility for precision mass measurements using highly charged ions", *Nucl. Instrum. Methods Phys. Res., Sect. A*, vol. 487, pp. 618-651, 2002. `doi:10.1016/S0168-9002(01)02178-7`

[15] S. Sturm *et al.*, "High-precision measurement of the atomic mass of the electron", *Nature*, vol. 506, pp. 467-470, 2014. `doi:10.1038/nature13026`

[16] F. Heiße *et al.*, "High-Precision Measurement of the Proton's Atomic Mass", *Phys. Rev. Lett.*, vol. 119, p. 033001, 2017. `doi:10.1103/PhysRevLett.119.033001`

[17] J. Repp *et al.*, "PENTATRAP: a novel cryogenic multi-Penning-trap experiment for high-precision mass measurements on highly charged ions", *Appl. Phys. B*, vol. 107, pp. 983–996, 2012. `doi:10.1007/s00340-011-4823-6`

[18] S. Ettenauer *et al.*, "First Use of High Charge States for Mass Measurements of Short-Lived Nuclides in a Penning Trap", *Phys. Rev. Lett.*, vol. 107, p. 272501, 2011. `doi:10.1103/PhysRevLett.107.272501`

[19] A. T. Gallant *et al.*, "Highly charged ions in Penning traps: A new tool for resolving low-lying isomeric states", *Phys. Rev. C*, vol. 85, p. 044311, 2012. `doi:10.1103/PhysRevC.85.044311`

[20] D. Frekers *et al.*, "Penning-trap Q-value determination of the ^{71}Ga$(\nu, e^-)^{71}$Ge reaction using threshold charge breeding of on-line produced isotopes", *Phys. Lett. B*, vol. 722, pp. 233-237, 2013. `doi:10.1016/j.physletb.2013.04.019`

[21] S. Ettenauer *et al.*, "Penning trap mass measurements utilizing highly charged ions as a path to benchmark isospin-symmetry breaking corrections in ^{74}Rb", *Phys. Rev. C*, vol. 91, p. 045504, 2015. `doi:10.1103/PhysRevC.91.045504`

[22] C. Babcock *et al.*, "Mass measurements of neutron-rich indium isotopes toward the $N = 82$ shell closure", *Phys. Rev. C*, vol. 97, p. 024312, 2018. `doi:10.1103/PhysRevC.97.024312`

[23] E. Leistenschneider, A. A. Kwiatkowski, and J. Dilling, "Vacuum requirements for Penning trap mass spectrometry with highly charged ions", *Nucl. Instrum. Methods Phys. Res., Sect. B*, vol. 463, pp. 496-498, 2020. `doi:10.1016/j.nimb.2019.03.047`

[24] G. Sikler *et al.*, "A high-current EBIT for charge-breeding of radionuclides for the TITAN spectrometer", *Eur. Phys. J. A - Hadrons and Nuclei*, vol. 25, p. 63, 2005. `doi:10.1140/epjad/i2005-06-072-6`

[25] A. Lapierre *et al.*, "The TITAN EBIT charge breeder for mass measurements on highly charged short-lived isotopes—First online operation", *Nucl. Instrum. Methods Phys. Res., Sect. A*, vol. 624, pp. 54–64, 2010. `doi:10.1016/j.nima.2010.09.030`

[26] Ruben Schupp, "Determination of beam properties of highly-charged ions extracted from TITAN's electron beam ion trap", M.Sc. thesis at University of Heidelberg, Germany, Winter 2016. `https://titan.triumf.ca/research/publications/RubenThesis2016.pdf`

[27] A. Kellerbauer *et al.*, "Buffer gas cooling of ion beams", *Nucl. Instrum. Methods Phys. Res., Sect. A*, vol. 469, pp. 276-285, 2001. `doi:10.1016/S0168-9002(01)00286-8`

[28] D. J. Wineland and W. M. Itano, "Laser cooling of atoms", *Phys. Rev. A*, vol. 20, p. 1521, 1979. `doi:10.1103/PhysRevA.20.1521`

[29] S. L. Rolston and G. Gabrielse, "Cooling antiprotons in an ion trap", *Hyperfine Interact.*, vol. 44, pp. 233–245, 1989. `doi:10.1007/BF02398673`

[30] J. Bernard *et al.*, "Electron and positron cooling of highly charged ions in a cooler Penning trap", *Nucl. Instrum. Methods Phys. Res., Sect. A*, vol. 532, pp. 224–228, 2004. `doi:10.1016/j.nima.2004.06.049`

[31] U. Chowdhury, "A Cooler Penning Trap to Cool Highly Charged Radioactive Ions and Mass Measurement of ^{24}Al", PhD thesis, University of Manitoba, 2016. `https://hdl.handle.net/1993/31511`

[32] Z. Ke *et al.*, "A cooler ion trap for the TITAN on-line trapping facility at TRIUMF", *Hyperfine Interact.*, vol. 173, pp. 103–111, 2006. `doi:10.1007/s10751-007-9548-x`

[33] V. V. Simon *et al.*, "A cooler Penning trap for the TITAN on-line trapping facility", *J. Phys.:Conf. Series*, vol. 312, p. 052024, 2011. `doi:10.1088/1742-6596/312/5/052024`

[34] S. F. Paul *et al.*, "Off-axis electron injection into a cooler Penning trap", *Hyperfine Interact.*, vol. 240, p. 50, 2019. `doi:10.1007/s10751-019-1587-6`

[35] D. Lascar *et al.*, "A novel transparent charged particle detector for the CPET upgrade at TITAN", *Nucl. Instrum. Methods Phys. Res., Sect. A*, vol. 868, pp. 133–138, 2017. `doi:10.1016/j.nima.2017.07.003`

[36] R. G. Greaves and C. M. Surko, "Inward Transport and Compression of a Positron Plasma by a Rotating Electric Field", *Phys. Rev. Lett.*, vol. 85, pp. 1883–1886, 2000. `doi:10.1103/PhysRevLett.85.1883`

[37] U. Chowdhury *et al.*, "A cooler Penning trap for the TITAN mass measurement facility", *AIP Conf. Proceedings*, vol. 1640, pp. 120-123, 2015. `doi:10.1063/1.4905408`

[38] S. F. Paul, "Off-axis electron injection into a cooler Penning trap", Master's thesis, University of Heidelberg, 2017.

[39] D. A. Dahl, "SIMION for the personal computer in reflection", *Int. J. Mass Spectrom.*, vol. 200, pp. 3-25, 2000. `doi:10.1016/S1387-3806(00)00305-5`

[40] B. Kootte *et al.*, "Quantification of the Electron Plasma in TItan's Cooler Penning Trap", in *Proc. Int. Workshop on Beam Cooling and Related Topics (COOL'15)*, Newport News, VA, USA, Sep. 2015, pp. 39–42. `doi:10.18429/JACoW-COOL2015-MOPF06`

[41] T. Mohamed *et al.*, "Fast electron accumulation and its mechanism in a harmonic trap under ultrahigh vacuum con-

ditions", *Phys. Plasmas*, vol. 18, p. 032507, 2011. `doi:10.1063/1.3562501`

[42] G. Maero *et al.*, "Stabilizing effect of a nonresonant radio frequency drive on the $m = 1$ diocotron instability", *Phys. Plasmas*, vol. 18, p. 032101, 2011. `doi:10.1063/1.3558374`

[43] F. Anderegg, "Waves in Non-Neutral Plasma", in *Physics with Trapped Charged Particles*, World Scientific, Singapore, 2014, pp. 173-193. `doi:10.1142/9781783264063_0006`

[44] N. E. Bradbury and R. A. Nielsen, "Absolute Values of the Electron Mobility in Hydrogen", *Phys. Rev.*, vol. 49, pp. 388–393, 1936. `doi:10.1103/PhysRev.49.388`

[45] J. R. Kimmel, F. Engelke, and R. N. Zare, "Novel method for the production of finely spaced Bradbury–Nielson gates", *Rev. Sci. Instrum.*, vol. 72, p. 4354, 2001. `doi:10.1063/1.1416109`